

Supplementary Material for
Production of methyl vinyl ketone and methacrolein via the hydroperoxyl
pathway of isoprene oxidation

by

Y. J. Liu (1), I. Herdlinger-Blatt (1,2), K. A. McKinney* (3), and S.T. Martin* (1,4)

(1) School of Engineering and Applied Sciences, Harvard University, Cambridge, Massachusetts,
USA

(2) Institute of Ion Physics and Applied Physics, University of Innsbruck, Innsbruck, Austria

(3) Department of Chemistry, Amherst College, Amherst, Massachusetts, USA

(4) Department of Earth and Planetary Sciences, Harvard University, Cambridge, Massachusetts,
USA

E-mail: kamckinney@amherst.edu

scot_martin@harvard.edu

<http://www.seas.harvard.edu/environmental-chemistry>

*To Whom Correspondence Should be Addressed

1 **A. Calibration of NO_x analyzer**

2 The instrument background in the absence of NO is obtained by converting NO to NO₂ in
3 the dry air from the pure air generator with additional ozone immediately before the NO detector.
4 The instrument sensitivity of NO was obtained by repeated calibration with NO standard diluted
5 with dry air and the instrumental sensitivity of NO₂ was obtained by converting NO to NO₂ with
6 additional ozone. The signals of NO and NO_x of the dry air from pure air generator had no
7 significant difference from instrument background.

8

9 **B. PTR-TOF-MS data analysis routine**

10 (1) Peak shape fitting

11 A numerical peak shape was generated for each 6-min sum spectrum as described in the
12 main text. No significant change of peak shape was observed within any one HDF file we have
13 collected so far, which was usually for less than 12 hr. Therefore, an averaged numeric peak
14 shape was used for each signal HDF file. The shape-fitting peaks used for the NO⁺ mode include
15 H₃O⁺ ($m/z=19.0178$ Th), NO₂⁺ ($m/z=45.9924$ Th) and C₅H₈⁺ ($m/z=68.0621$ Th, only for chamber
16 steady state conditions). For the H₃O⁺ mode, H₃¹⁸O⁺ ($m/z=21.0221$ Th), NO⁺ ($m/z=29.9974$ Th)
17 and H₅O¹⁸O⁺ ($m/z=39.0327$ Th) were used.

18 (2) Mass calibration

19 Using a generated peak shape, a peak fitting algorithm was then applied to a list of mass
20 calibration peaks to optimize the time-of-flight of their peak maximum. In the case of NO⁺ mode,
21 the mass calibration peaks included H₃O⁺, NO₂⁺, H₂NO₂⁺ ($m/z=48.0080$ Th), and C₅H₈⁺ (only for
22 chamber steady state conditions). For H₃O⁺ mode, the mass calibration peaks included H₃O¹⁸⁺,
23 NO⁺, H₅O¹⁸O⁺, NO₂⁺ ($m/z=45.9924$ Th) and H₇O₃⁺ ($m/z=55.0390$ Th). The relationship of the

24 time-of-flight and the mass-to-charge ratio (m/z) was calculated according to the following
25 equation by fitting the coefficients α and β :

$$m/z = \left(\frac{\text{TOF} - \beta}{\alpha}\right)^2$$

26 The mass calibration peaks covered only the m/z range below 70 Th, but the m/z of the
27 ions generated from isoprene oxidation products were expected to be as high as 120 Th. To
28 examine whether this could be a source of inaccuracy for mass calibration, an external mass
29 calibration compound, 1,4-dichlorobenzene, was therefore added for a check. The product ions
30 of 1,4-dichlorobenzene $\text{C}_6\text{H}_4\text{Cl}_2^+$ ($m/z=145.968$) and $\text{C}_6\text{H}_4\text{Cl}_2\text{NO}^+$ ($m/z=175.966$) were used for
31 the mass calibration at the NO^+ mode. For the H_3O^+ mode, $\text{C}_6\text{H}_5\text{Cl}_2^+$ ($m/z=146.976$) was used.
32 The deviation of the mass calibration curve obtained with and without 1,4-dichlorobenzene ions
33 was below 5 ppm for both modes in the m/z range below 150 Th. Therefore, the mass calibration
34 without adding external calibration compound worked well for the interested mass range.

35 (3) Peak assignment

36 With a good mass calibration and a well-defined peak shape, we then assigned ion
37 formula for the peaks in the full m/z range. A pre-existing ion list was created, containing all
38 possible combination of C, H, O, N and their important isotopes with an m/z below 200 Th. A
39 target peak was first fitted using the ion with an m/z ratio most close to the peak maximum. If
40 there was a significant residual peak left, a second ion with an m/z ratio most close to the residual
41 peak maximum was added into the fitting procedure. The peak assignment process was done
42 manually to avoid missing any shoulder peaks.

43 (4) Signal analysis

44 For signal analysis, peak fitting algorithm was applied on the target peaks using pre-
45 assigned ion formulas. The resulting peak signal (cps) were normalized to a primary ion signal of
46 10^6 cps without transmission correction (cps \rightarrow ncps), as described by de Gouw et al. (2003)

47

48 **C. Wall-loss experiment**

49 Separate chamber experiments were performed to test the wall loss of isoprene, MVK
50 and MACR. The target species were continuously injected into the chamber bag using syringe
51 pump until their concentrations got stabilized. All the inflows and injection were then stopped
52 for 2 hrs. At the same time the gas-phase concentrations of the target species were continuously
53 measured. No drop in the signal of isoprene, MVK and MACR was observed, suggesting
54 negligible wall loss at steady state.

55

56 **D. Dependence of the sensitivities on the E/N ratio**

57 The influence of electric field energy (E/N ratio) on the sensitivity response of isoprene,
58 MVK and MACR for the NO^+ mode is illustrated in Figure S3. The sensitivities of all the three
59 compounds decreased with increasing E/N . The ratio of $\text{C}_4\text{H}_6\text{O}\cdot\text{NO}^+/\text{C}_4\text{H}_5\text{O}^+$ ion signals for
60 MACR also decreased with increasing E/N . To ensure better separation of MACR from MVK
61 which only produced $\text{C}_4\text{H}_6\text{O}\cdot\text{NO}^+$ ions and at the same time high sensitivities for both species,
62 the drift tube voltage was kept at 300 V and drift tube temperature at 60 °C during chamber
63 experiments, corresponding to an E/N ratio of 68 Td.

64 As shown in Figure S3, at lower E/N ratios smaller changes in the sensitivity of isoprene
65 were observed. A similar trend was also observed by Knighton et al. (2009) and Karl et al.
66 (2012). As a comparison point, the sensitivity of isoprene was 14.6 ncps/ppb at an E/N ratio of

67 104 Td in the present work. It is very close to the value obtained by Karl et al. using a similar
 68 PTR-TOF-MS instrument, 12.5 ncps/ppb (estimated from Figure 3 in their paper), but much
 69 lower than the value obtained by Knighton et al. using a PTR-QMS instrument, 21 ncps/ppb
 70 (estimated from Figure 4 in their paper).

71

72 E. Equations for concentration quantification

73 Concentrations of isoprene, MVK, and MACR in the chamber outflow were quantified
 74 using the following equations:

$$75 \quad c[\text{Isoprene}] = \frac{i[\text{C}_5\text{H}_8^+] - i[\text{C}_5\text{H}_8^+]_{bg}}{s[\text{C}_5\text{H}_8^+, \text{Isoprene}]} \quad (\text{S1})$$

$$76 \quad c[\text{MACR}] = \frac{i[\text{C}_4\text{H}_5\text{O}^+] - i[\text{C}_4\text{H}_5\text{O}^+]_{bg} - 0.011 (i[\text{C}_5\text{H}_8] - i[\text{C}_5\text{H}_8]_{bg})}{s[\text{C}_4\text{H}_5\text{O}^+, \text{MACR}]} \quad (\text{S2})$$

$$77 \quad c[\text{MVK}] = \frac{i[\text{C}_4\text{H}_6\text{O} \cdot \text{NO}^+] - i[\text{C}_4\text{H}_5\text{O}^+]_{bg} - s[\text{C}_4\text{H}_6\text{O} \cdot \text{NO}^+, \text{MACR}] c[\text{MACR}]}{s[\text{C}_4\text{H}_6\text{O} \cdot \text{NO}^+, \text{MVK}]} \quad (\text{S3})$$

78 where $c[\text{M}]$ is the concentration of species M in the chamber air; $i[\text{N}^+]$ (cps) is the measured
 79 signal of ion N^+ for chamber air; $i[\text{N}^+]_{bg}$ (cps) is the measured background signal of ion N^+ using
 80 zero air; and $s[\text{N}^+, \text{M}]$ (cps/ppb) is the sensitivity of compound M with respect to ion N^+ , as
 81 determined by calibration. A small amount of $\text{C}_4\text{H}_5\text{O}^+$ was also produced from isoprene (1.1% of
 82 C_5H_8^+ ion), which was taken into account in converting ion signals to concentrations.

83

84 F. Equation for yield determination with ozone correction

$$85 \quad 0 = \left(Y_{\text{MVK}} k_1 c[\text{OH}]_{ss} c[\text{C}_5\text{H}_8]_{ss} + Y_{\text{MVK}, \text{O}_3} k_3 c[\text{O}_3]_{ss} c[\text{C}_5\text{H}_8]_{ss} \right)_{sources} - \left(k_2 c[\text{OH}]_{ss} c[\text{MVK}]_{ss} + k_4 c[\text{O}_3]_{ss} c[\text{MVK}]_{ss} + \frac{1}{\tau} c[\text{MVK}]_{ss} + k_{wall} c[\text{MVK}]_{ss} \right)_{sinks} \quad (\text{S4})$$

86

$$Y_{MVK} = \frac{(k_2 c[\text{OH}]_{ss} + k_4 c[\text{O}_3]_{ss} + 1/\tau + k_{wall}) c[\text{MVK}]_{ss}}{k_1 c[\text{OH}]_{ss} c[\text{C}_5\text{H}_8]_{ss}} - \frac{Y_{MVK,O_3} k_3 c[\text{O}_3]_{ss} c[\text{C}_5\text{H}_8]_{ss}}{k_1 c[\text{OH}]_{ss} c[\text{C}_5\text{H}_8]_{ss}} \quad (\text{S5})$$

87

$$0 = \left(\frac{1}{\tau} c[\text{C}_5\text{H}_8]_{in} \right)_{sources} - \left(k_1 c[\text{OH}]_{ss} c[\text{C}_5\text{H}_8]_{ss} + k_3 c[\text{O}_3]_{ss} c[\text{C}_5\text{H}_8]_{ss} + \frac{1}{\tau} c[\text{C}_5\text{H}_8]_{ss} \right)_{sinks} \quad (\text{S6})$$

88 where k_3 and k_4 are the reaction rate coefficients of isoprene and MVK with O_3 , respectively,

89 Y_{MVK,O_3} is the yield of MVK from ozonolysis of isoprene.

90

91 G. Uncertainty Evaluation

92 The uncertainties listed in Table 1 in the main text represent standard deviations
 93 estimated using Monte Carlo methods. To evaluate the uncertainty of the concentrations, the ion
 94 signals and the sensitivities listed in Equation S1-S3 were used as input parameters with assumed
 95 normal distributions. The means and standard deviations of input ion signals were estimated
 96 using measurements in 10 min. The means and standard deviations of input sensitivities were
 97 shown in Table 2 in the main text.

98 To evaluate the uncertainty of the yields, inflow concentrations of isoprene, steady-state
 99 concentration of isoprene, MVK, MACR, and ozone, and residence time were considered as
 100 input variables with assumed normal distributions. The mean and standard deviations of the
 101 concentrations of the organic species were evaluated as discussed above. Standard deviations of
 102 10% and 20% were assumed for ozone concentration and residence time, respectively.

103

104 H. Dependence of the interference on instrumental conditions

105 To understand whether thermal decomposition of the condensing compounds, possibly
106 ISOPOOH, occurred in the instrument (60 °C), the change in ion signals of steady-state chamber
107 air was monitored at a low drift tube temperature of 30 °C as the inlet temperature was varied
108 from 30 °C to 80 °C. The trap temperature was kept at 25 °C. The residence time of the sample
109 air in the drift tube and in the inlet line was comparable (60-80 ms). No significant change in ion
110 signals was observed, suggesting that thermal decomposition of other oxidation products inside
111 the instrument did not contribute to the ions at the same m/z ratio as MVK and MACR product
112 ions.

113 Measurements of steady-state chamber air have been made at various E/N ratios in both
114 NO^+ and H_3O^+ mode. The apparent concentrations of isoprene, MVK, and MACR were
115 quantified with respective calibrations at each E/N ratio. Here the apparent concentrations are
116 defined as the equivalent concentrations of isoprene, MVK, and MACR assuming no
117 interference compounds. As shown in the top panels of Figure S6, the apparent MVK and
118 MACR concentrations were independent on E/N ratio in the range of 15-70 Td in the NO^+ mode
119 and 20-120 Td in the H_3O^+ mode. This observation indicates that the fragmentation of the
120 interference compounds was not very sensitive to the collision energy we used.

121 As shown in the bottom panels of Figure S6, the apparent concentrations of MVK and
122 MACR showed some decrease as the temperature of the drift tube decreased. The apparent
123 concentrations were quantified using respective calibrations at each temperature. The decrease of
124 the apparent concentration of MVK + MACR at the NO^+ mode was bigger than that at the H_3O^+
125 mode. This observation suggests that fragmentation of the condensing compounds was thermally
126 driven, which seems inconsistent with the independence of the E/N ratio. Further investigation is
127 hence needed to fully understand the mechanism.

128

129 **Reference**

130 de Gouw, J., Warneke, C., Karl, T., Eerdekens, G., van der Veen, C., and Fall, R.: Sensitivity and
131 specificity of atmospheric trace gas detection by proton-transfer-reaction mass spectrometry, *Int.*
132 *J. Mass. Spectrom.*, 223-224, 365-382, 2003.

133 Karl, T., Hansel, A., Cappellin, L., Kaser, L., Herdlinger, I., and Jud, W.: Selective
134 measurements of isoprene and 2-methyl-3-buten-2-ol based on NO^+ ionization mass
135 spectrometry, *Atmos. Chem. Phys. Discuss.*, 12, 19349-19370, doi: 10.5194/acpd-12-19349-
136 2012, 2012.

137 Knighton, W. B., Fortner, E. C., Herndon, S. C., Wood, E. C., and Miake-Lye, R. C.: Adaptation
138 of a proton transfer reaction mass spectrometer instrument to employ NO^+ as reagent ion for the
139 detection of 1,3-butadiene in the ambient atmosphere, *Rapid. Commun. Mass. Sp.*, 23, 3301-
140 3308, doi: 10.1002/rcm.4249, 2009.

141 **List of Figures**

142 **Figure S1.** Schematic diagram of the experimental set-up.

143 **Figure S2.** Mechanism of isoprene oxidation to produce ISOPOOH and IEPOX as represented in
144 MCM v3.2. Branching ratios to specific products are shown in parentheses.

145 **Figure S3.** Dependence of sensitivity of isoprene, MVK, and MACR on E/N ratios at NO^+ mode.
146 The drift tube temperature was kept at 70 °C.

147 **Figure S4.** Change in the signal of selected ion for steady-state chamber air measured with H_3O^+
148 reagent ions as the trap temperature dropped from room temperature to -40 °C in discrete steps.
149 Left column shows the time series of temperature (top) and of ion signals (bottom) in
150 Experiment #1 under HO_2 -dominant conditions, and right column shows results for Experiment
151 #7 under NO -dominant conditions. Solid line and dashed line in the bottom panels represent the
152 ion signal of C_5H_9^+ and $\text{C}_4\text{H}_7\text{O}^+$, respectively.

153 **Figure S5.** Change in the equivalent concentrations of the interference compounds to MVK and
154 MACR with chamber residence time. The equivalent concentration of MVK/MACR
155 interferences is defined as the difference of MVK/MACR concentration at the trap temperature
156 of +25 °C and that at -40 °C. The residence time of reference experiment was 3.7 hr.

157 **Figure S6.** Change in the apparent concentrations of isoprene, MVK, and MACR at steady state
158 with the E/N ratios (top) and the drift-tube temperature (bottom) at both NO^+ (left) and H_3O^+
159 (right) mode. For H_3O^+ mode, the sum of MVK and MACR concentration was calculated using
160 the average sensitivity of MVK and MACR. The trap temperature was kept at +25 °C. For the
161 experiments at various E/N ratios, the drift tube temperature was kept on 70 °C and the drift tube
162 voltage was varied. For the experiments at various temperatures of the drift tube, the drift tube
163 voltage was 300 V and 520 V for the NO^+ and H_3O^+ modes, respectively.

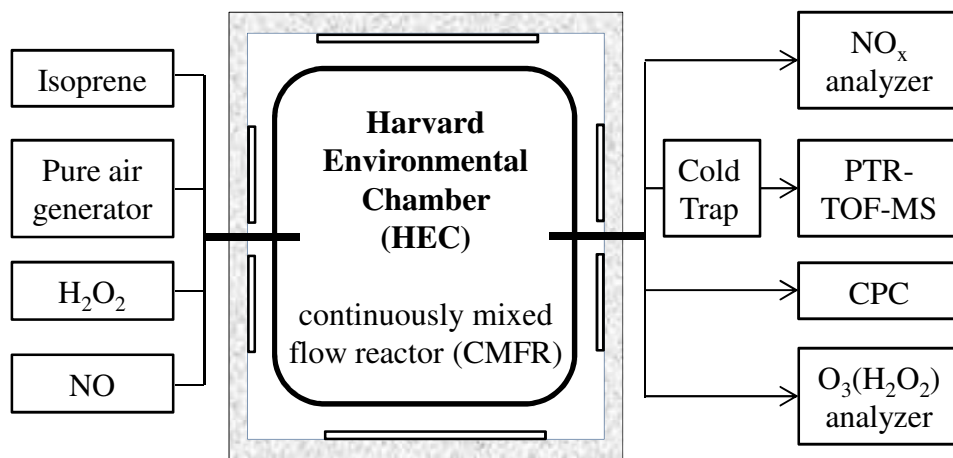


Figure S1

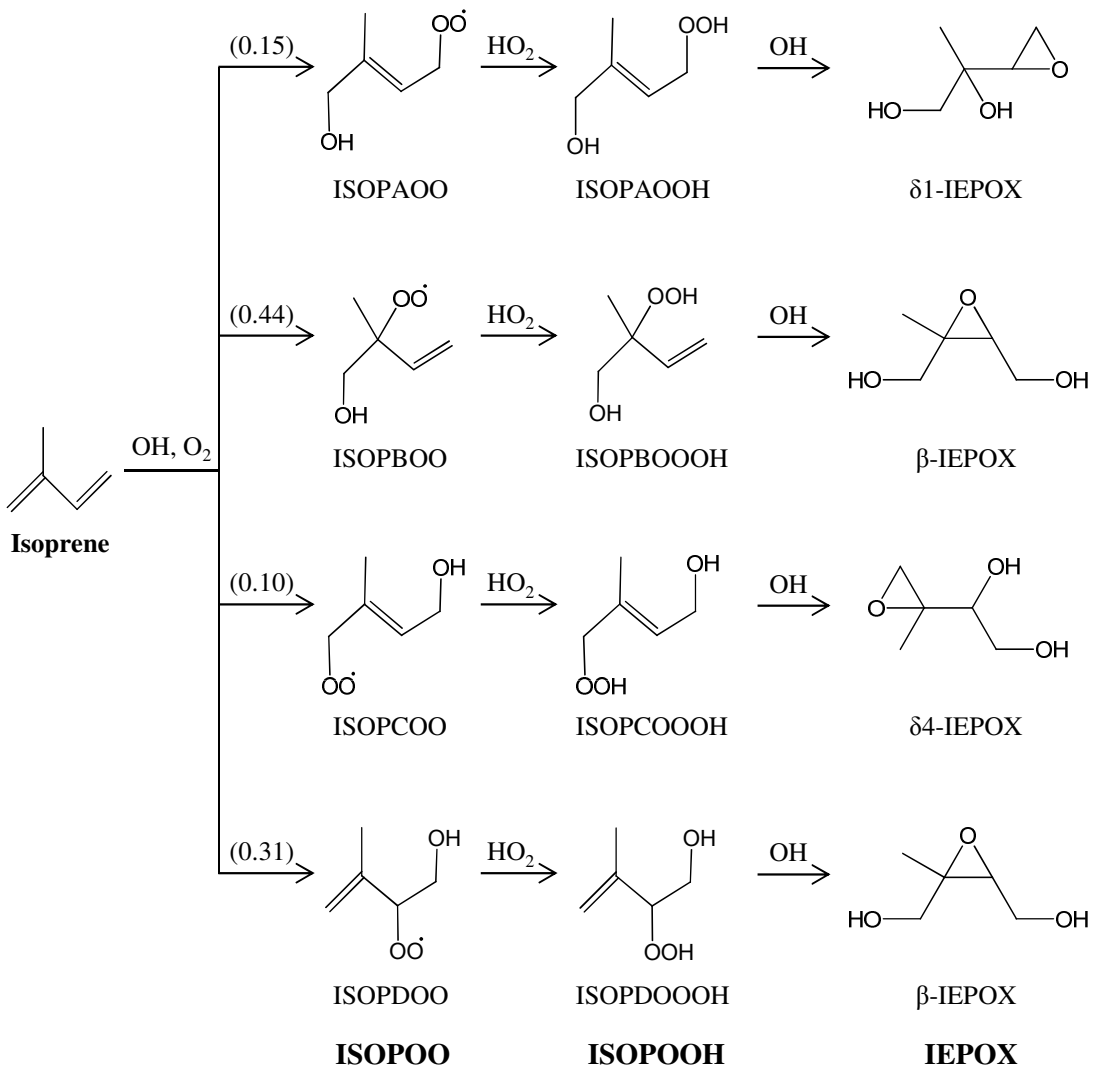


Figure S2

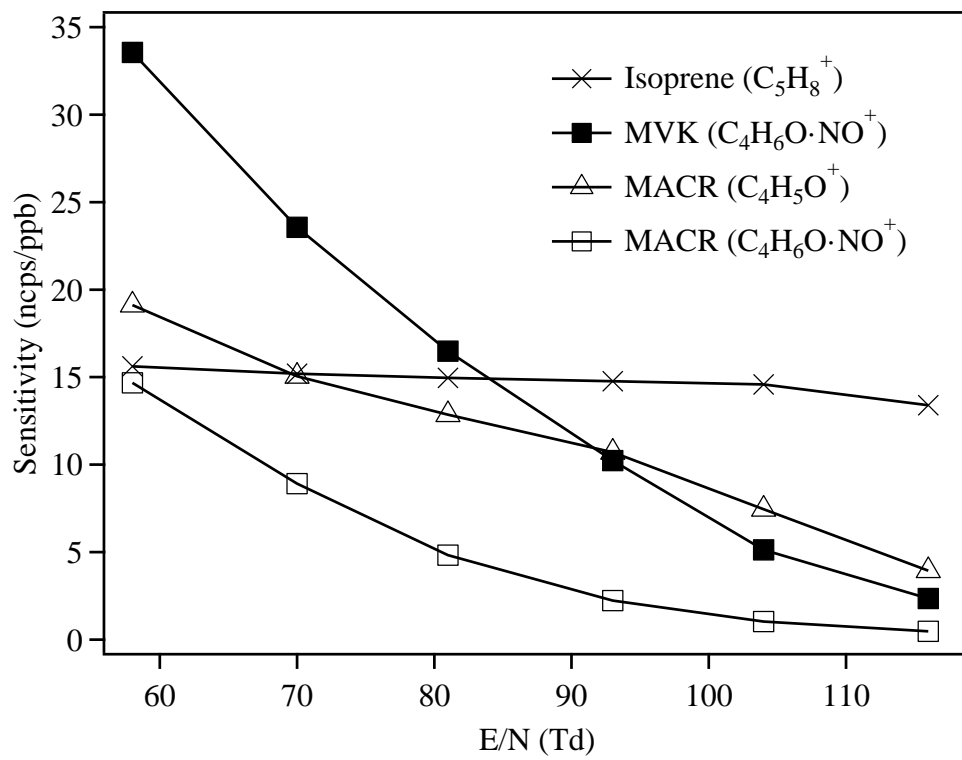


Figure S3

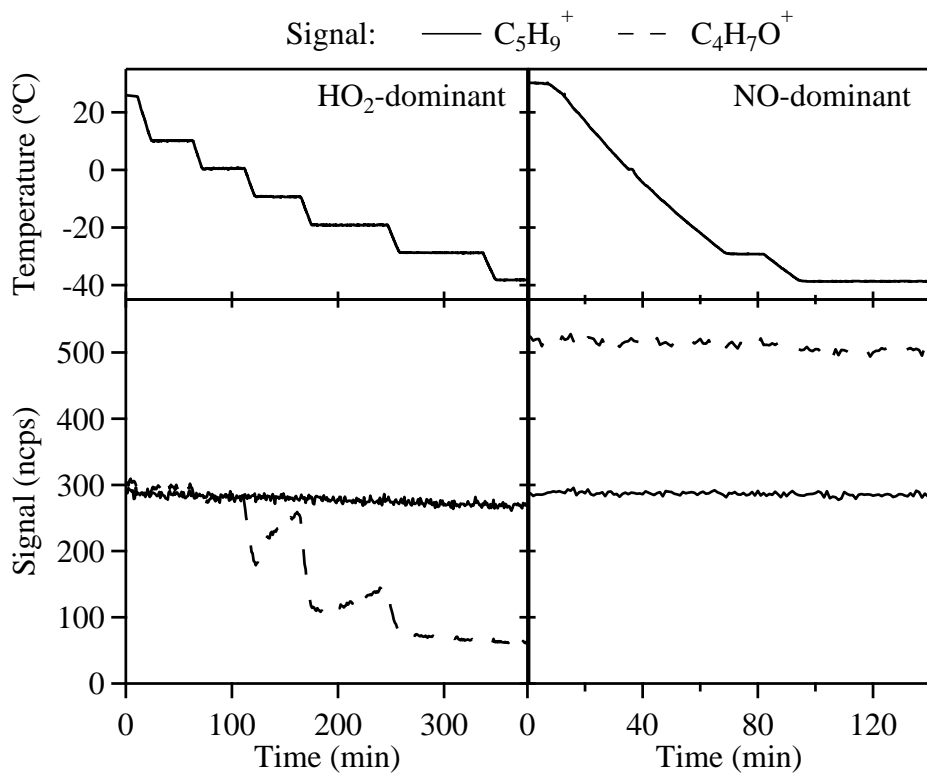


Figure S4

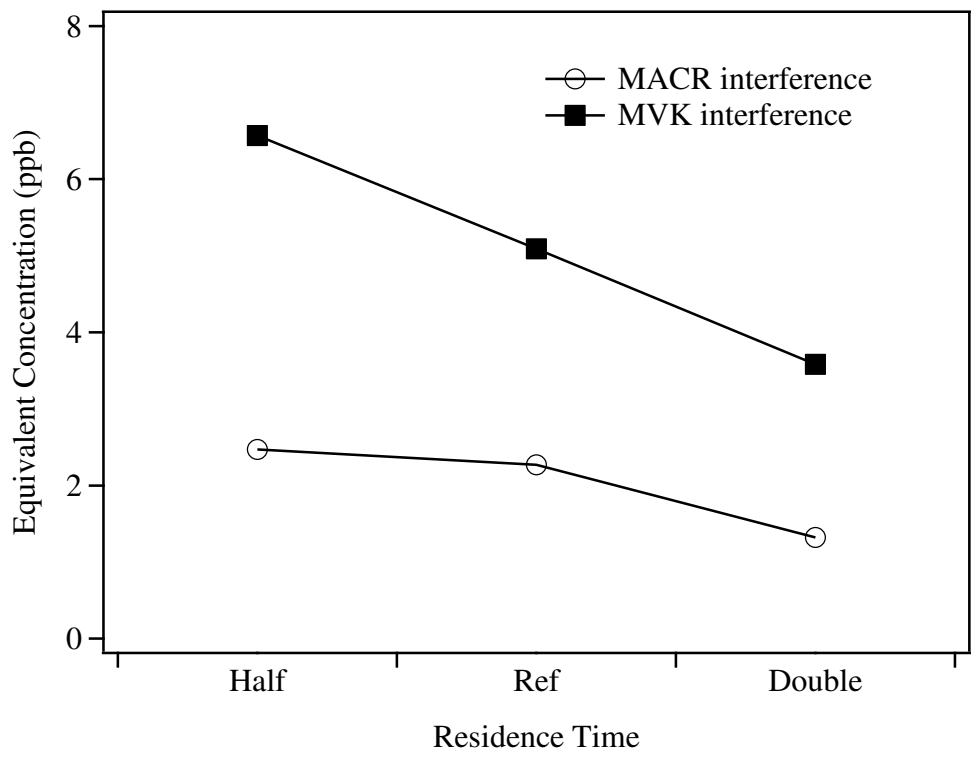


Figure S5

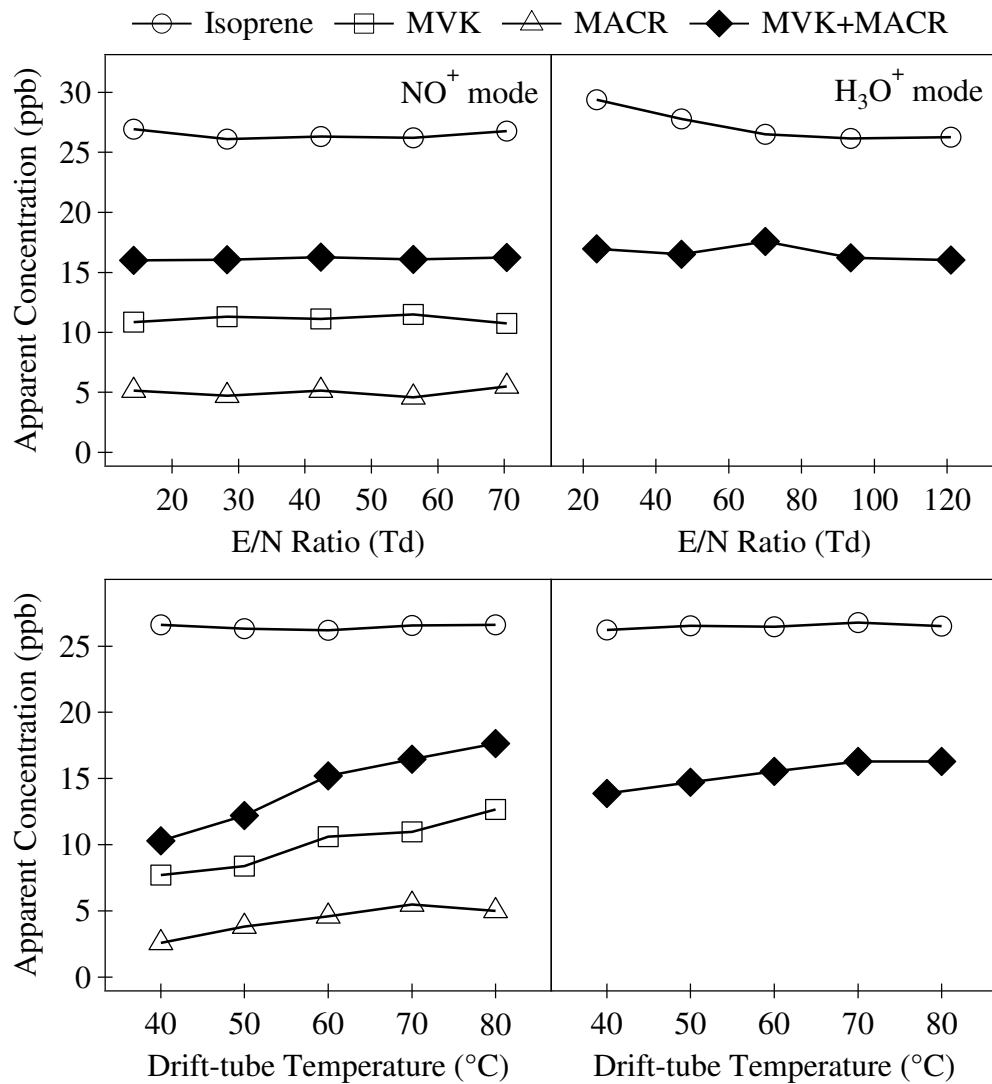


Figure S6